

# A New Measurement of the $\Xi_c^+$ Lifetime

The FOCUS Collaboration

J. M. Link<sup>a</sup>, M. Reyes<sup>a</sup>, P. M. Yager<sup>a</sup>, J. C. Anjos<sup>b</sup>,  
I. Bediaga<sup>b</sup>, C. Göbel<sup>b</sup>, J. Magnin<sup>b</sup>, A. Massafferri<sup>b</sup>,  
J. M. de Miranda<sup>b</sup>, I. M. Pepe<sup>b</sup>, A. C. dos Reis<sup>b</sup>, S. Carrillo<sup>c</sup>,  
E. Casimiro<sup>c</sup>, A. Sánchez-Hernández<sup>c</sup>, C. Uribe<sup>c</sup>, F. Vázquez<sup>c</sup>,  
L. Cinquini<sup>d</sup>, J. P. Cumalat<sup>d</sup>, B. O'Reilly<sup>d</sup>, J. E. Ramirez<sup>d</sup>,  
E. W. Vaandering<sup>d</sup>, J. N. Butler<sup>e</sup>, H. W. K. Cheung<sup>e</sup>,  
I. Gaines<sup>e</sup>, P. H. Garbincius<sup>e</sup>, L. A. Garren<sup>e</sup>, E. Gottschalk<sup>e</sup>,  
P. H. Kasper<sup>e</sup>, A. E. Kreymer<sup>e</sup>, R. Kutschke<sup>e</sup>, S. Bianco<sup>f</sup>,  
F. L. Fabbri<sup>f</sup>, A. Zallo<sup>f</sup>, C. Cawfield<sup>g</sup>, D. Y. Kim<sup>g</sup>,  
A. Rahimi<sup>g</sup>, J. Wiss<sup>g</sup>, R. Gardner<sup>h</sup>, A. Kryemadhi<sup>h</sup>,  
Y. S. Chung<sup>i</sup>, J. S. Kang<sup>i</sup>, B. R. Ko<sup>i</sup>, J. W. Kwak<sup>i</sup>, K. B. Lee<sup>i</sup>,  
H. Park<sup>i</sup>, G. Alimonti<sup>j</sup>, M. Boschini<sup>j</sup>, G. Chiodini<sup>j</sup>,  
P. D'Angelo<sup>j</sup>, M. DiCorato<sup>j</sup>, P. Dini<sup>j</sup>, M. Giammarchi<sup>j</sup>,  
P. Inzani<sup>j</sup>, F. Leveraro<sup>j</sup>, S. Malvezzi<sup>j</sup>, D. Menasce<sup>j</sup>,  
M. Mezzadri<sup>j</sup>, L. Milazzo<sup>j</sup>, L. Moroni<sup>j</sup>, D. Pedrini<sup>j</sup>,  
C. Pontoglio<sup>j</sup>, F. Prelz<sup>j</sup>, M. Rovere<sup>j</sup>, S. Sala<sup>j</sup>,  
T. F. Davenport III<sup>k</sup>, L. Agostino<sup>l</sup>, V. Arena<sup>l</sup>, G. Boca<sup>l</sup>,  
G. Bonomi<sup>l</sup>, G. Gianini<sup>l</sup>, G. Liguori<sup>l</sup>, M. M. Merlo<sup>l</sup>,  
D. Pantea<sup>l</sup>, S. P. Ratti<sup>l</sup>, C. Riccardi<sup>l</sup>, I. Segoni<sup>l</sup>, P. Vitulo<sup>l</sup>,  
H. Hernandez<sup>m</sup>, A. M. Lopez<sup>m</sup>, H. Mendez<sup>m</sup>, L. Mendez<sup>m</sup>,  
A. Mirles<sup>m</sup>, E. Montiel<sup>m</sup>, D. Olaya<sup>m</sup>, A. Paris<sup>m</sup>, J. Quinones<sup>m</sup>,  
C. Rivera<sup>m</sup>, W. Xiong<sup>m</sup>, Y. Zhang<sup>m</sup>, J. R. Wilson<sup>n</sup>, K. Cho<sup>o</sup>,  
T. Handler<sup>o</sup>, R. Mitchell<sup>o</sup>, D. Engh<sup>p</sup>, M. Hosack<sup>p</sup>,  
W. E. Johns<sup>p</sup>, M. Nehring<sup>p</sup>, P. D. Sheldon<sup>p</sup>, K. Stenson<sup>p</sup>,  
M. Webster<sup>p</sup>, M. Sheaff<sup>q</sup>

<sup>a</sup>University of California, Davis, CA 95616

<sup>b</sup>Centro Brasileiro de Pesquisas Físicas, Rio de Janeiro, RJ, Brasil

<sup>c</sup>CINVESTAV, 07000 México City, DF, Mexico

<sup>d</sup>University of Colorado, Boulder, CO 80309

<sup>e</sup>Fermi National Accelerator Laboratory, Batavia, IL 60510

<sup>f</sup>*Laboratori Nazionali di Frascati dell'INFN, Frascati, Italy I-00044*

<sup>g</sup>*University of Illinois, Urbana-Champaign, IL 61801*

<sup>h</sup>*Indiana University, Bloomington, IN 47405*

<sup>i</sup>*Korea University, Seoul, Korea 136-701*

<sup>j</sup>*INFN and University of Milano, Milano, Italy*

<sup>k</sup>*University of North Carolina, Asheville, NC 28804*

<sup>l</sup>*Dipartimento di Fisica Nucleare e Teorica and INFN, Pavia, Italy*

<sup>m</sup>*University of Puerto Rico, Mayaguez, PR 00681*

<sup>n</sup>*University of South Carolina, Columbia, SC 29208*

<sup>o</sup>*University of Tennessee, Knoxville, TN 37996*

<sup>p</sup>*Vanderbilt University, Nashville, TN 37235*

<sup>q</sup>*University of Wisconsin, Madison, WI 53706*

---

## Abstract

A precise determination of the charm-strange baryon  $\Xi_c^+$  lifetime is presented. The data were accumulated by the Fermilab high-energy photoproduction experiment FOCUS. The measurement is made with 300  $\Xi_c^+ \rightarrow \Xi^- \pi^+ \pi^+$  decays, 130  $\Xi_c^+ \rightarrow \Sigma^+ K^- \pi^+$  decays, 45  $\Xi_c^+ \rightarrow p K^- \pi^+$  decays and 58  $\Xi_c^+ \rightarrow \Lambda^0 K^- \pi^+ \pi^+$  decays. The  $\Xi_c^+$  lifetime is measured to be  $0.439 \pm 0.022 \pm 0.009$  ps.

---

## 1 Introduction

The lifetime hierarchy of the weakly decaying charm mesons is well established [1]. However, the pattern of the predicted lifetimes for the weakly decaying charm baryons agrees only qualitatively with experimental results [2,3]. The  $\Lambda_c^+$  lifetime is known to an accuracy of  $\sim 5\%$  [4,5], but the others, ( $\Xi_c^+$ ,  $\Xi_c^0$ ,  $\Omega_c^0$ ), have uncertainties on the order of 20%. Interestingly, baryon sector lifetime measurements provide information on quark interference and W-exchange. The essential difference from the mesons is that W-exchange among the valence quarks of the baryon is neither color nor helicity suppressed. The measured  $\Xi_c^+$  lifetime is larger than theory predicts, but there is a large experimental uncertainty [6,7]. A more precise measurement could be conclusive in testing predictions in this sector.

In the FOCUS spectrometer<sup>1</sup> high energy photons with  $\langle E \rangle \approx 180$  GeV interact in a segmented BeO target to produce charmed particles. Charged

---

<sup>1</sup> FOCUS spectrometer is an upgraded version of the Fermilab E687 spectrometer [8].

particles are tracked in the target region by two silicon vertex detectors which provide excellent vertex separation between the production and decay vertices. The average proper time resolution is  $\approx 50$  fs for the modes used in this analysis. Downstream tracking and momentum measurement is performed by a system of five multiwire proportional chambers (MWPC) and two magnets of opposite polarity. The upstream magnet (M1) is positioned downstream of the silicon detectors and in front of the MWPC system. The second magnet (M2) lies between the third and fourth MWPC stations. Charged particle identification is provided by three multicell threshold Čerenkov counters and two muon systems. One hadronic and two electromagnetic calorimeters are used to measure particle energy.

## 2 Reconstruction of hyperons $\Xi^-$ and $\Sigma^+$

A detailed description of the  $\Xi^-$  and  $\Sigma^+$  reconstruction can be found elsewhere [9]. The  $\Xi^-$  decays into  $\Lambda^0\pi^-$ , with the  $\Lambda^0$  being reconstructed, if possible, through the decay  $\Lambda^0 \rightarrow p\pi^-$ .<sup>2</sup> The  $\Xi^-$ 's are reconstructed according to where and how the decay occurs. We consider four categories: Type1 where the  $\Xi^-$  decays promptly without leaving a track in the silicon detectors; Type2 where the  $\Xi^-$  decays after passing through the silicon and the  $\Lambda^0$  daughter is fully reconstructed; MV decays, which are topologically identical to Type2 decays, but are reconstructed from the intersection of the three MWPC tracks from the  $\Xi^-$  decay with the  $\Xi^-$  silicon track; Kink decays where the  $\Xi^-$  passes through the silicon and the  $\Lambda^0$  daughter is not reconstructed. If a  $\Xi^-$  candidate is reconstructed both as Type2 and MV, then we choose the Type2 to avoid duplication. In Kink type decays, due to the failure to reconstruct the  $\Lambda^0$ , there is normally a two-fold ambiguity in the determination of the momentum. However, by requiring that the decay occurs in M1 we remove this ambiguity. Our data is composed of 9% Type1, 66% Type2, 6% MV and 19% Kink. We have more than one million reconstructed  $\Xi^-$ 's in all four types.

The  $\Sigma^+$  baryon can decay into  $p\pi^0$  or  $n\pi^+$ . Each channel is studied separately. The reconstruction is similar to the Kink category described above. For the neutron in the  $\Sigma^+ \rightarrow n\pi^+$  decay we require  $0.3 < E/p < 2.0$ , where  $E$  is the energy deposited in the calorimeters and  $p$  is the reconstructed momentum. For the  $\Sigma^+ \rightarrow p\pi^0$  decays, the protons must be positively identified in the Čerenkov system. As in the case of Kink type  $\Xi^-$ 's, we have a two-fold ambiguity in the determination of the  $\Sigma^+$  momentum. This ambiguity can be partially removed for the  $\Sigma^+ \rightarrow n\pi^+$  decay by using the location of energy deposition in the calorimeters.

---

<sup>2</sup> Throughout this paper, the charge conjugate state is implied whenever the decay mode of a particular charge is stated.

### 3 Reconstruction of $\Xi_c^+$ candidates

The  $\Xi_c^+$  candidate is reconstructed using a candidate driven vertexing algorithm [8]. A  $\Xi_c^+$  candidate vertex is formed using the silicon track information of the decay daughters when available. This (secondary) vertex is required to have a confidence level (CL) above a value optimized for each topology reconstructed. We construct a seed track using the momentum vector of the  $\Xi_c^+$  candidate and intersect it with at least two other tracks to form a primary vertex. This primary vertex is required to have a confidence level greater than 1% and to be in the target material to within 3 units of the error in the primary vertex position ( $TGM < 3$ ). We tighten this requirement to  $TGM < 0$  for the cases where the  $\Xi^-$  or  $\Sigma^+$  are partially reconstructed. Other cuts used to optimize the signal are the confidence level that any other track originates from the secondary vertex (ISO2), the error in the proper time ( $\sigma_t$ ), and the significance of separation of the primary and secondary vertices ( $L/\sigma_L$ ). Čerenkov particle identification is accomplished by constructing  $\chi^2$  like variables for the different particle hypotheses [10]. Briefly, we compute likelihoods for the various stable particle hypotheses  $e$ ,  $\pi$ ,  $K$  and  $p$ . The pion consistency of a track is defined by a requirement on  $\Delta W_\pi = W_{\min} - W_\pi$ , where  $W_\pi$  is the negative log likelihood of the pion hypothesis and  $W_{\min}$  is the minimum negative log likelihood of the other three hypotheses. Similarly, we define  $\Delta W_K = W_\pi - W_K$  and  $\Delta W_p = W_\pi - W_p$  for use in identifying kaons and protons. We require  $\Delta W_\pi > -6$  and  $\Delta W_K > 2$  for pion and kaon identification in all modes. Additional particle identification is mode dependent and is described below. The resulting invariant mass distributions are shown in Figure 1; the combined plot is shown in Figure 4(a).

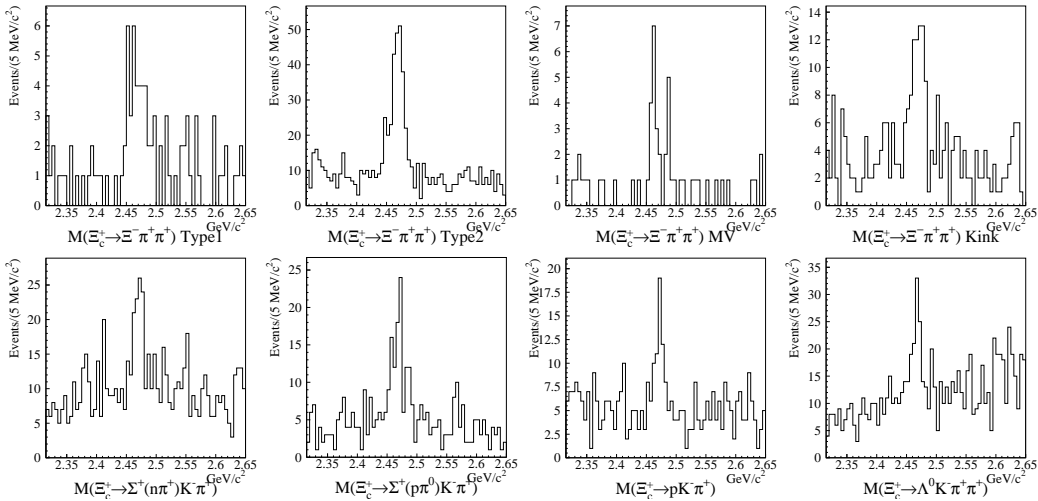


Fig. 1.  $\Xi_c^+ \rightarrow \Xi^- \pi^+ \pi^+$  (4 reconstruction methods),  $\Sigma^+ K^- \pi^+$  (2 decay modes),  $p K^- \pi^+$  and  $\Lambda^0 K^- \pi^+ \pi^+$  invariant mass distributions with cuts as described in the text.

### 3.1 $\Xi_c^+ \rightarrow \Xi^- \pi^+ \pi^+$ selection criteria

The secondary vertex is required to have a CL greater than 2% except for Type1  $\Xi^-$  where we require it to be greater than 10%. For Kink type decays we require that  $\sigma_t$  be less than 0.06 ps and that ISO2 be less than 0.01%. The additional cuts are necessary since we cannot make an invariant mass cut on  $\Xi^-$  candidates of this type. We demand that  $L/\sigma_L$  be greater than 4.

### 3.2 $\Xi_c^+ \rightarrow \Sigma^+ K^- \pi^+$ selection criteria

If there is an ambiguity in the  $\Sigma^+$  momentum determination we resolve it as follows. First, we select the higher momentum solution when the difference in the masses calculated using each solution is less than 30 MeV/ $c^2$ . When the difference is greater than 30 MeV/ $c^2$  we reject a solution candidate if the other  $\Xi_c^+ \rightarrow \Sigma^+ K^- \pi^+$  mass is within  $2.5\sigma$  of the nominal  $\Xi_c^+$  mass. For a small fraction of cases this can lead to rejecting or accepting both solutions. Resolving the ambiguity in this way may create a bias and we have studied this as a possible source of systematic uncertainty. The CL of the secondary vertex must be greater than 2% and we require  $\sigma_t$  to be less than 0.07 ps. We ask that  $L/\sigma_L$  be greater than 7.

### 3.3 $\Xi_c^+ \rightarrow p K^- \pi^+$ selection criteria

We identify protons by requiring that  $\Delta W_p > 10$  and that the proton hypothesis is favored over the kaon hypothesis by two units of likelihood i.e.  $W_K - W_p > 2$ . We demand that  $W_p - W_K > 0$  for the kaon candidate. For pion candidates we require the momentum to be greater than 5 GeV/ $c$ . The secondary vertex must have a CL greater than 15% and ISO2 less than 0.01%. To reduce combinatorial background, the  $\Xi_c^+$  candidate momentum is required to be less than 120 GeV/ $c$ . Long lifetime backgrounds from charmed mesons, where one particle is misidentified, are removed by making an invariant mass cut. In this way we eliminate contamination from the decays  $D^+ \rightarrow K^- \pi^+ \pi^+$ ,  $D^+(D_s^+) \rightarrow K^- K^+ \pi^+$  and  $D^0 \rightarrow K^+ K^-$ . Finally, cuts of  $\sigma_t$  less than 0.08 ps and  $L/\sigma_L$  greater than 7 are applied.

### 3.4 $\Xi_c^+ \rightarrow \Lambda^0 K^- \pi^+ \pi^+$ selection criteria

We select  $\Lambda^0$  candidates which decay downstream of the silicon vertex detector. To reduce contamination from  $K_S \rightarrow \pi^+ \pi^-$  decays, we require  $\Delta W_p > 8$  for

the proton in the  $\Lambda^0$  decay. The secondary vertex must have a CL greater than 15% and ISO2 less than 0.01%. Cuts of  $\sigma_t$  less than 0.10 ps and  $L/\sigma_L$  greater than 4 are applied.

#### 4 Lifetime technique.

We perform a binned maximum likelihood fit [11] to extract the lifetime of the  $\Xi_c^+$  from the aforementioned decay channels. We fit the reduced proper time ( $t'$ ) distribution, defined as  $t' = (L - N\sigma_L)/\beta\gamma c$  where  $N$  is the vertex detachment cut,  $\beta c$  is the particle velocity and  $\gamma$  is the Lorentz boost factor to the  $\Xi_c^+$  center of mass frame. The  $t'$  distribution for  $\Xi_c^+$  is of the form  $e^{-t'/\tau}$ , where  $\tau$  is the lifetime of the  $\Xi_c^+$ . A fit is made to the  $t'$  distribution for events which lie within  $\pm 2\sigma$  of the  $\Xi_c^+$  mass, where  $\sigma$  is  $\sim 8$  MeV/ $c^2$  for the  $\Xi_c^+ \rightarrow \Lambda^0 K^- \pi^+ \pi^+$  channel and  $\sim 10$  MeV/ $c^2$  otherwise. The background is assumed to have the same lifetime behavior in the signal region and in the sidebands which are 4–12 $\sigma$  away from the peak. Taking  $S$  as the number of signal events in the mass region and  $B$  as the total number of background events in the same region, the expected number of events  $n_i$  in the  $i^{\text{th}}$  reduced proper time bin centered at  $t'$  is given by:

$$n_i = S \frac{f(t'_i) e^{-t'_i/\tau}}{\sum_i f(t'_i) e^{-t'_i/\tau}} + B \frac{b_i}{\sum_i b_i} \quad (1)$$

where  $b_i$  describes the background reduced proper time evolution as estimated from sidebands and  $f(t'_i)$  is a correction function, which takes into account the effects of spectrometer acceptance, analysis cut efficiencies, and absorption of the particles as a function of the reduced proper time. In Figure 2 we plot the correction function for each decay mode. The large corrections in some modes at low reduced proper time are due to the suppression of short lived decays by our selection cuts. The likelihood is constructed from the product of the Poisson probability of observing  $s_i$  events when  $n_i$  are expected with the Poisson probability of observing  $\sum b_i$  background events when  $4B$  are expected. The factor of 4 accounts for the fact that the sideband region is four times wider than the signal region. The likelihood takes the form:

$$\mathcal{L} = \left( \prod_i \frac{n_i^{s_i} e^{-n_i}}{s_i!} \right) \times \left( \frac{(4B)^{\sum_i b_i} e^{-4B}}{(\sum_i b_i)!} \right) \quad (2)$$

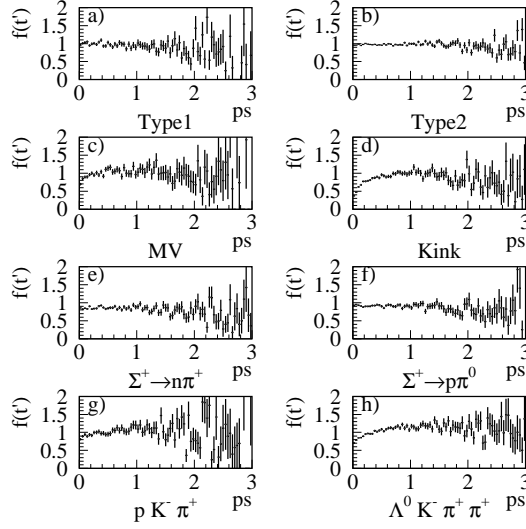


Fig. 2. Lifetime correction functions for the different decay modes and topologies described earlier.

The combined likelihood function is given by the product of the eight likelihoods as shown in Eq. (3).

$$\begin{aligned}
 \mathcal{L}_{\Xi_c^+} = & \mathcal{L}_{\text{Type1}}^{\Xi^- \pi^+ \pi^+} \times \mathcal{L}_{\text{Type2}}^{\Xi^- \pi^+ \pi^+} \times \mathcal{L}_{\text{MV}}^{\Xi^- \pi^+ \pi^+} \times \mathcal{L}_{\text{Kink}}^{\Xi^- \pi^+ \pi^+} \\
 & \times \mathcal{L}_{\Sigma^+(n\pi^+)}^{\Sigma^+ K^- \pi^+} \times \mathcal{L}_{\Sigma^+(p\pi^0)}^{\Sigma^+ K^- \pi^+} \times \mathcal{L}_{pK^- \pi^+} \times \mathcal{L}_{\Lambda^0 K^- \pi^+ \pi^+}
 \end{aligned} \quad (3)$$

There are nine parameters in the fit, one parameter for the lifetime  $\tau$  and eight parameters for the backgrounds one for each decay type. Our result for the  $\Xi_c^+$  lifetime with statistical errors is  $0.435 \pm 0.022$  ps.

## 5 Systematic Studies

We compute the lifetime using several different  $L/\sigma_L$  cuts. The results are shown in Figure 3(a). Systematic effects were studied by computing the lifetimes of data samples split by individual  $\Xi^-$  topologies and modes. The results are shown in Figure 3(b). All variations are consistent within statistical uncertainties and do not contribute to a systematic uncertainty. We have investigated systematic effects due to the  $t'$  resolution by examining the variance in the fitted lifetime for different  $t'$  bin size, by reducing the  $t'$  range for the fit from 3 to 2 ps and by excluding the lowest  $t'$  bin from the fit. Uncertainties in the measurement of particle momenta can lead to a systematic shift in the reduced proper time. Our studies show this shift to be  $4 \pm 2$  fs. The final quoted value is adjusted by this amount and a systematic uncertainty of 2 fs is included in the final systematic uncertainty. The treatment of the two solution ambiguity in the  $\Sigma^+ K^- \pi^+$  mode creates a small bias in the measured

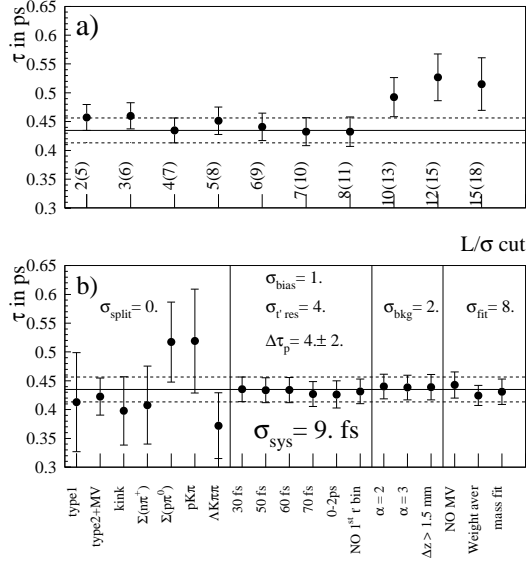


Fig. 3. a) Lifetime stability versus  $L/\sigma_L$ ; in parenthesis is the  $L/\sigma_L$  cut used for  $\Sigma^+K^-\pi^+$  and  $pK^-\pi^+$ . b) lifetime measurements for systematic studies. The solid line represent the central value with the dotted lines showing the extent of the statistical error at  $L/\sigma_L > 4(7)$ .

Table 1

Contributions to the systematic uncertainty.

Contribution	Uncertainty (fs)
$\Xi_c^+$ Momentum	$\pm 2$
two solution bias	$\pm 1$
Split sample	0
$t'$ Resolution	$\pm 4$
Background	$\pm 2$
Fit variant	$\pm 8$
Total	$\pm 9$

lifetime due to an overestimation of the background in the signal region. This effect is less than 1 fs on the total lifetime. Systematic effects due to the background were investigated by varying the width of the sideband regions, and by altering the background level by imposing a minimum separation between the primary and secondary vertices of 1.5 mm. The variance from these tests is added to the systematic uncertainty. We tested different fit conditions; excluding MV type decays from the lifetime fit, taking the weighted average of the split samples, and using a combined fit to the mass shape and reduced proper time of  $\Xi_c^+ \rightarrow \Sigma^+K^-\pi^+$  as an alternative method of treating the two solution ambiguity. The systematic uncertainty due to the variation in fit conditions is taken to be the sample variance since we consider all of the measurements to



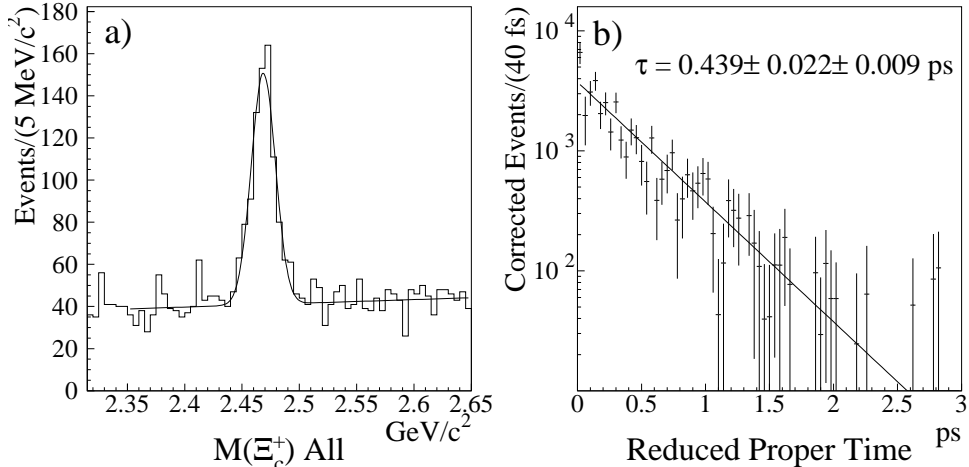


Fig. 4. a) The invariant mass for the combined sample. b) The combined lifetime fit of the  $\Xi_c^+$  modes with a background subtracted, Monte Carlo corrected, reduced proper time distribution.

be equally valid. The systematic contribution is found to be 8 fs.

The components of the systematic error are presented in Table 1. Adding these contribution in quadrature gives a total systematic uncertainty of 9 fs. Figure 4(b) shows the background subtracted, Monte Carlo corrected, reduced proper time distribution for the  $\Xi_c^+$  signal.

## 6 Summary

We have measured the  $\Xi_c^+$  using four decay modes which occur in eight different topologies with a combined sample of  $532.4 \pm 30.4$  events. We find the lifetime to be  $0.439 \pm 0.022 \pm 0.009$  ps where the first error is statistical and the second is systematic. Our result is compared with other experimental values in Table 2. Our measurement uncertainty is a factor of two better than those of the current world average [1]. As discussed in the introduction, theoretical models predict the lifetime hierarchy of the charmed baryons. A number of authors [2,15–17] predict that  $\tau(\Xi_c^+) > \tau(\Lambda_c^+)$  where the inequality represents a factor of about 1.3. Using the  $\Lambda_c^+$  lifetime average of PDG, CLEO, and SELEX [1,4,5] ( $0.1916 \pm 0.0054$  ps) and the  $\Xi_c^+$  lifetime reported in this paper, a ratio  $\tau(\Xi_c^+)/\tau(\Lambda_c^+) = 2.29 \pm 0.14$ , is obtained. Our well measured ratio is significantly different from predictions of order 1.3.

Table 2  
 $\Xi_c^+$  lifetime measurements

Experiment	Lifetime (ps)	Events	Year
WA62 [12]	$0.48^{+0.21+0.20}_{-0.15-0.15}$	53	1985
E400 [13]	$0.40^{+0.18}_{-0.12} \pm 0.10$	102	1987
ACCMOR (NA32)[14]	$0.20^{+0.11}_{-0.06}$	6	1989
E687 [7]	$0.41^{+0.11}_{-0.08} \pm 0.02$	30	1993
E687 [6]	$0.34^{+0.07}_{-0.05} \pm 0.02$	56	1998
PDG (average) [1]	$0.33^{+0.06}_{-0.04}$	–	2000
This Measurement	$0.439 \pm 0.022 \pm 0.009$	532	2001

## 7 Acknowledgments

We wish to acknowledge the assistance of the staffs of Fermi National Accelerator Laboratory, the INFN of Italy, and the physics departments of the collaborating institutions. This research was supported in part by the U. S. National Science Foundation, the U. S. Department of Energy, the Italian Istituto Nazionale di Fisica Nucleare and Ministero dell’Università e della Ricerca Scientifica e Tecnologica, the Brazilian Conselho Nacional de Desenvolvimento Científico e Tecnológico, CONACyT-México, the Korean Ministry of Education, and the Korean Science and Engineering Foundation.

## References

- [1] D. E. Groom et al. (Particle Data Group), *Eur. Phys. J.* **C15**, 1 (2000).
- [2] B. Guberina and B. Melic, *Eur. Phys. J.* **C2**, 697 (1998), [hep-ph/9704445](#).
- [3] G. Bellini, I. I. Y. Bigi, and P. J. Dornan, *Phys. Rept.* **289**, 1 (1997).
- [4] A. H. Mahmood et al. (CLEO), *Phys. Rev. Lett.* **86**, 2232 (2001), [hep-ex/0011049](#).
- [5] A. Kushnirenko et al. (SELEX), *Phys. Rev. Lett.* **86**, 5243 (2001), [hep-ex/0010014](#).
- [6] P. L. Frabetti et al. (E687), *Phys. Lett.* **B427**, 211 (1998).
- [7] P. L. Frabetti et al. (E687), *Phys. Rev. Lett.* **70**, 1381 (1993).
- [8] P. L. Frabetti et al. (E687), *Nucl. Instrum. Meth.* **A320**, 519 (1992).
- [9] J. M. Link et al. (FOCUS) (2001a), accepted for publication *Nucl. Instrum. Meth. A* (FERMILAB-Pub-01/244-E), [hep-ex/0109028](#).

- [10] J. M. Link et al. (FOCUS) (2001b), accepted for publication Nucl. Instrum. Meth. A (FERMILAB-Pub-01/243-E), [hep-ex/0108011](#).
- [11] P. L. Frabetti et al. (E687), Phys. Lett. **B263**, 584 (1991).
- [12] S. F. Biagi et al., Phys. Lett. **B150**, 230 (1985).
- [13] P. Coteus et al., Phys. Rev. Lett. **59**, 1530 (1987).
- [14] S. Barlag et al. (ACCMOR), Phys. Lett. **B233**, 522 (1989).
- [15] I. I. Y. Bigi (1996), talk given at Workshop on Heavy Quarks at Fixed Target (HQ 96), St. Goar, Germany, 3-6 Oct 1996 (UND-HEP-96-BIG06), [hep-ph/9612293](#).
- [16] B. Blok and M. A. Shifman (1991), talk given at 3rd Workshop on the Tau-Charm Factory, Marbella, Spain, 1-6 Jun 1993 (TPI-MINN-93-55-T, UMN-TH-1227-93, TECHNION-PH-93-41), [hep-ph/9311331](#).
- [17] H.-Y. Cheng, Phys. Rev. **D56**, 2783 (1997), [hep-ph/9704260](#).